RSC Advances

PAPER

View Article Online
View Journal | View Issue

A used battery supported Ag catalyst for efficient oxidation of alcohols and carbon oxide†

Cite this: *RSC Adv.*, 2014, **4**, 25384

Junjie Mao, Guofeng Zhao, Dingsheng Wang* and Yadong Li

Received 28th February 2014
Accepted 22nd April 2014

DOI: 10.1039/c4ra01786b

www.rsc.org/advances

Green-recycling of existing waste is significant in green chemistry. Herein, we show that used batteries can be applied as cheap and viable supports for silver catalysts and used for gas-phase alcohol and CO oxidation. The catalyst Ag-9/Mn_3O_4 (Ag-loading: 9 wt%) is efficient for oxidizing acyclic, benzylic and polynary alcohols. For instance, Ag-9/Mn_3O_4 can oxidize cyclohexanol into cyclohexanone with 86% conversion and 88% selectivity. In addition, a special synergistic effect between the Ag and the Mn_3O_4 was revealed, which is particularly valuable for the design of composite catalysts. The facile strategy employed in this study can be expanded to the fabrication of other catalysts with the green reuse of used batteries as supports.

Introduction

With ever-increasing serious environmental and energy issues, sustainable harvesting that begins with extracting resources from earth using cost-effective techniques which minimize negative impacts is becoming more and more important.[1] Taking battery recycling as an example, the global per capita per annum battery consumption of 330 g can leave a massive residue of untreated battery waste, which not only pollutes the environment but also leads to great energy waste.[2,3] Thus, establishing a battery-recycle-system is of significance to sustainable development.

The selective oxidation of alcohols to the corresponding carbonyl compounds is of interest due to its fundamental importance for laboratory and industrial manufacturing.[4–8] Traditionally, alcohols are oxidized in solution using a variety of metal based homogeneous catalysts. However, these methods are usually associated with low reaction rates, difficult catalyst–solvent separation, and serious toxicity issues, which hamper their wide applications. Thus, a highly selective and recyclable "green" catalyst for solvent free alcohol oxidation is required for the large scale synthesis of carbonyl compounds.[9,10] Moreover, the development of reusable catalysts for the gas-phase aerobic oxidation of alcohols is also valuable to the fields of organic synthesis and green chemistry.

Recently, silver nanoparticle (Ag NP) catalysts supported on activated carbon, oxides, or polymers have been proved to be advantageous over noble metal NPs for the oxidation of alcohols owing to their higher selectivity, resistance to leaching, and lower cost.[11,12] Moreover, it is well recognized that the selection of a suitable scaffold to support the Ag NPs has a critical role in determining the catalytic activity and selectivity. Thus, developing novel recycled materials as supports for Ag NPs for highly efficient and selective alcohol oxidation could be important.

Among the various metal oxides that can support Ag NPs as catalysts, manganese oxide has been widely used as a stoichiometric oxidant for hydrocarbons or alcohols as well as a support or promoter for metal or metal oxide catalysts.[13–15] For example, Li *et al.* reported a low-temperature carbon monoxide (CO) oxidation reaction using Ag/MnO_2 as a catalyst,[16] in which the MnO_2 enhanced the catalytic ability of the Ag NPs significantly. However, to the best of our knowledge, manganese oxide supported Ag NPs for gas-phase catalytic alcohol oxidation hasn't been thoroughly investigated.

Here, we have developed a novel catalyst using a used battery to support Ag NPs. The *in situ* reduction results in an even dispersion of Ag NPs on the MnO_2 support. The as-prepared Ag/Mn_3O_4 catalyst (transformation from Ag/MnO_2, using weight hourly space velocity (WHSV) = 20 h^{-1} and molar ratio of O_2 to alcoholic hydroxyl (O_2/ol) = 0.6 at 280 °C) is an efficient catalyst for the transformation of a diverse range of alcohols to the corresponding carbonyl compounds under solvent-free conditions. For cyclohexanol, the catalyst Ag-9/Mn_3O_4 (Ag-loading: 9 wt%) delivered a high conversion of 86% and a cyclohexanone selectivity of 88% at a temperature of 280 °C. Moreover, the results based on comparable catalysts and characterization indicate that the formation of a Ag–support interface and the interactions therein contribute to the high activity for alcohol and CO oxidation.

Department of Chemistry, Tsinghua University, Beijing 100084, P. R. China. E-mail: wangdingsheng@tsinghua.edu.cn

† Electronic supplementary information (ESI) available: Experimental details, XRD, TEM, N_2 adsorption–desorption isotherms and pore size distribution curves of samples; oxidation of various alcohols over the catalysts. See DOI: 10.1039/c4ra01786b

Results and discussion

The original powder (MnO_x) mixture from used batteries was firstly characterized by using XRD (Fig. S1†). The XRD patterns of the MnO_x indicated the presence of manganese oxide, zinc hydroxide, and iron compounds, which was further confirmed by ICP analysis. After the purification of MnO_x, pure MnO_2 was successfully obtained (JCPDS 24-0735). Moreover, other crystallized impurities, such as zinc and iron compounds in the original powder, were not observed. The structure of the recycled MnO_2 was characterized by TEM (Fig. S2†).

Fig. 1A shows the XRD patterns of the Ag/MnO_2, which indicate that the MnO_2 phase was unchanged after the Ag deposition. Moreover, metallic silver diffraction peaks were not observed for the catalysts with low Ag-loading (3–5%), but then appeared in the catalysts with high Ag-loading from 7% to 11%. The Ag/MnO_2 catalysts were then characterized by TEM (Fig. S3†), and the Ag NPs were found to be highly dispersed on the surface of the MnO_2 support. Taking the Ag-9/MnO_2 catalyst as an example, the Ag particle size is between 6–8 nm according to the particle size distribution (PSD) histogram, with a mean size of 6.99 nm (Fig. 2A inset). The *d*-spacing for adjacent lattice fringes measured from several different regions was 2.36 Å (Fig. 2B), which is close to that of the (111) planes of a face-centered cubic (fcc) Ag crystal. The high-angle annular dark-field scanning TEM (HAADF-STEM) image (Fig. 2C) further confirmed that the Ag NPs are well-dispersed on the MnO_2 surface. The energy-dispersive X-ray spectroscopy (EDS) mapping profile (Fig. 2D) further manifested the homogeneous distribution of Ag, Mn, and O in the Ag-9/MnO_2 nanocrystals. The above results indicate that the employed *in situ* reduction method is simple and facile for the fabrication of the Ag/MnO_2 catalyst. N_2 adsorption–desorption isotherms (Fig. S4†) indicated the mesoporous structure of all the samples, with Barrett–Joyner–Halenda (BJH) pore sizes of 12.88 nm for MnO_x, 32.60 nm for MnO_2, and 21.67 nm for Ag-9/MnO_2 (Fig. S4†, insets). BET measurements indicated that the MnO_x and MnO_2 have BET surface areas of 22.98 $m^2 g^{-1}$ and 41.56 $m^2 g^{-1}$, respectively, while the deposition of Ag NPs onto the MnO_2 surface slightly reduced the surface area of MnO_2 to 35.53 $m^2 g^{-1}$.

Cyclohexanone is an important raw chemical for the organic syntheses of caprolactam (for nylon 6) and adipic acid, widely used in the leather industry, and in degreasing agents and detergents.[17,18] Many efforts have been devoted to the conversion of cyclohexanol to cyclohexanone in liquid phase.[19,20] However, gas-phase oxidation as a promising route for further industrial application has been less investigated.[21] Here, the selective gas-phase oxidation of cyclohexanol over the Ag/Mn_3O_4 catalyst was thoroughly investigated.

In recent years, silver based heterogeneous catalysts have been developed for alcohol oxidation. Therefore, an initial experiment was carried out over the catalyst Ag/ZrO_2, and the cyclohexanol conversion was 53% with a high WHSV of 20 h^{-1} at 280 °C (entry 3 in Table 1), but with a selectivity of 62%, which has restricted the manufacture of highly pure cyclohexanone using this route. The relatively efficient alcohol oxidation using Ag-based catalysts prompted us to develop new systems to further enhance the catalytic performance of alcohol oxidation. Manganese oxide has a superior ability to activate and supply oxygen, and has been extensively investigated as an excellent support. A series of MnO_2 catalysts with different silver loadings were synthesized and employed for the oxidation of alcohols.

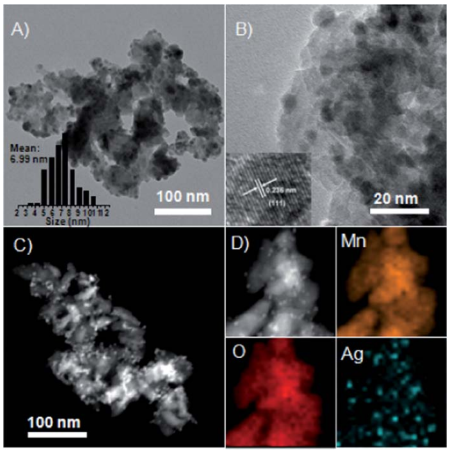

Fig. 2 (A) TEM image of Ag-9/MnO_2 (inset is the Ag particle size distribution), (B) HRTEM images of Ag-9/MnO_2 (inset is the enlarged HRTEM image of Ag nanocrystals), (C) HAADF-STEM image of Ag-9/MnO_2 nanocrystals, and (D) HAADF-STEM image together with the EDX mapping of Ag-9/MnO_2 nanocrystals.

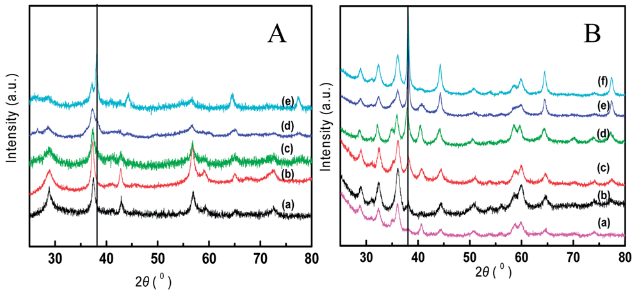

Fig. 1 (A) XRD patterns of the samples before pre-activation treatment: (a) Ag-3/MnO_2, (b) Ag-5/MnO_2, (c) Ag-7/MnO_2, (d) Ag-9/MnO_2, (e) Ag-11/MnO_2; (B) XRD patterns of the catalysts after pre-activation: (a) Mn_3O_4, (b) Ag-3/Mn_3O_4, (c) Ag-5/Mn_3O_4, (d) Ag-7/Mn_3O_4, (e) Ag-9/Mn_3O_4, (f) Ag-11/Mn_3O_4. Pre-activation conditions: catalysts for the gas-phase oxidation of cyclohexanol were pre-activated using WHSV = 20 h^{-1} and O_2/ol = 0.6 at 280 °C in advance.

Table 1 Oxidation of cyclohexanol over the various pre-activated catalysts. Calcination temperature: 400 °C

Entry	Catalysts	$T_{Reaction}$ (°C)	Conversion (%)	Selectivity (%)
1	Ag-9/Al_2O_3	280	27	74
2	Ag-9/ZnO	280	45	58
3	Ag-9/ZrO_2	280	53	62
4	Ag-9/SiO_2	280	22	23
5	Ag-9/TiO_2	280	58	52
6	Ag-9/Fe_2O_3	280	75	60
7	Ag-9/Mn_3O_4	280	86	88

We first studied the efficiency of the MnO_2-supported silver catalysts with varying silver loading for solvent-free alcohol oxidation by molecular oxygen. Of particular significance is the observation that the catalytic activity of the Ag/MnO_2 catalysts for the gas-phase oxidation of cyclohexanol was enhanced after pre-activation using WHSV $= 20\ h^{-1}$ and O_2/ol $= 0.6$ at 280 °C. The XRD results indicated that after pre-activation, Ag/MnO_2 was transformed into Ag/Mn_3O_4 (Fig. 1B). Fig. 3A and B show the cyclohexanol conversion and cyclohexanone selectivity of the reaction over the pre-activated Ag/Mn_3O_4 catalysts with various Ag-loadings at 280 °C using a WHSV of 20 h^{-1} and O_2/ol of 0.6. Ag-loading has a strong influence on the catalytic performance. Increasing the Ag-loading from 0 to 7 wt% significantly enhanced the conversion from 42% to 82% and the selectivity from 45% to 77%. However, further increasing the Ag-loading to 11 wt% caused a slight decrease of both the conversion and the selectivity, maybe due to the increased size of the Ag NPs. Among all of the pre-activated catalysts, the most active was the pre-activated Ag-9/Mn_3O_4, for which the conversion was further increased to 86% with a selectivity of 88%. The detectable byproducts included cyclohexene, cyclohexane, benzene and small amounts of CO_x. These catalytic results clearly revealed that the cyclohexanol conversion and cyclohexanone selectivity over the Ag-9/Mn_3O_4 catalyst are about two times higher than that of Mn_3O_4 at the same temperature, which demonstrates that the Ag embedment modification of the Mn_3O_4 remarkably enhanced the low-temperature activity. It should be pointed out that, unless otherwise specified, the reaction results reported in the following parts are all based on the pre-activated catalysts. More interestingly, if the raw materials from waste batteries were simply washed just with drinking water, satisfactory catalytic performance was also obtained, with a conversion of 82% and a selectivity of 83% at 280 °C, thus greatly increasing the potential for industrial applications and in other fields.

A key factor that must be considered for heterogeneous catalysts is the possibility of the active components vaporizing during the reaction, thereby leading to catalyst deactivation or, in the worst case, to the formation of an active gas-phase homogeneous catalyst. The reactor below the catalyst bed was washed with strong acid composed of HCl and HNO_3 ($HCl : HNO_3$ of 3 : 1 (vol : vol)). The ICP results of the obtained organic-product and the acid-washing liquid solution showed the absence of Ag and Mn, indicating the thermal stability of the Ag-9/Mn_3O_4 catalyst for alcohol oxidation. Additionally, many reported results show that the catalyst support plays an important, sometimes crucial role in determining the catalyst performance. In order to investigate the effect of the support on catalytic performance, we prepared a series of comparable catalysts on several other supports, including ZrO_2, ZnO, Al_2O_3, SiO_2 TiO_2 and Fe_2O_3. All of the catalysts were evaluated for the oxidation of cyclohexanol, with the results listed in Table 1. Generally, most catalysts demonstrated a much lower cyclohexanol conversion, indicating that the Mn_3O_4 is an effective support of the silver catalyst for cyclohexanol oxidation.

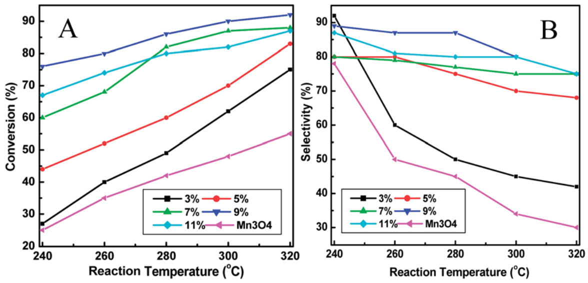

Fig. 3 Catalytic performance of the catalysts with various Ag loadings. (A) Cyclohexanol conversion and (B) cyclohexanone selectivity over the pre-activated Ag/Mn_3O_4 catalysts. (The gas-phase oxidation of cyclohexanol was performed using O_2/ol of 0.6 and WHSV of 20 h^{-1}. Catalyst: 0.1 g; quartz sands: 0.2 g (100–150 mesh).)

The reaction conditions such as the reaction temperature and WHSV on the performance of Ag-9/Mn_3O_4 catalyst for the selective gas-phase oxidation of cyclohexanol were elaborately investigated, and the results are shown in Fig. 3 and S5.† As shown in Fig. 3A and B, the as-obtained Mn_3O_4 and pre-activated Ag-9/Mn_3O_4 catalyst provided quite different conversion behavior on changing the reaction temperature. For Mn_3O_4 in the gas-phase oxidation of cyclohexanol, increasing the temperature from 240 °C to 320 °C gave a small increase in cyclohexanol conversion, which was accompanied by an obvious reduction in selectivity for the target products from 78% to 30%. When silver NPs were supported on the MnO_2 to form the Ag-9/Mn_3O_4 catalyst, the increase of reaction temperature from 240 °C to 320 °C caused the conversion to increase from 76% to 92% while the selectivity decreased slightly to 75%.

In particular, a high selectivity for the formation of cyclohexanone with a conversion of 86% was obtained using the Ag-9/Mn_3O_4 catalyst at 280 °C. However, pure Mn_3O_4 showed very poor activity for this reaction under the same conditions (conversion: ~42%, selectivity: ~45%, main by-product: cyclohexene). At 280 °C, on increasing the WHSV from 5 to 20 h^{-1}, the conversion of cyclohexanol was decreased from 92% to 86% under O_2/ol of 0.6 (Fig. S5†). On increasing the WHSV from 20 to 30 h^{-1}, the cyclohexanol conversion sharply decreased to 50% with the selectivity almost unchanged, which indicated that the resistance time was not sufficient for enough reactant and product molecules to react with O_2 thereby leading to the decrease in conversion. Considering a balance between high product yield and low temperature, the optimal operational parameters are a WHSV of 20 h^{-1}, with an O_2/ol of 0.6 at 280 °C.

Table S1† compiles the catalytic results for the oxidation of a range of structurally different alcohols (such as straight-chain, benzylic and polynary alcohols) over the pre-activated Ag-9/Mn_3O_4. The experimental results show that the catalysis was influenced by the structure of the alcohol substrates. It is apparent that the Ag-9/Mn_3O_4 catalyst showed a higher activity for aromatic alcohols than for aliphatic ones. The pre-activated Ag-9/Mn_3O_4 could selectively oxidize 1-phenylethanol to acetophenone with a high conversion of 95% at 250 °C but only converted 23% of 2-phenylethanol, even at the higher temperature of 280 °C. This difference may be due to the specific interactions of this substrate with the active site. In the oxidation of 1-octanol and 2-octanol, the primary linear aliphatic alcohol (1-ol) was oxidized with a conversion of 40% and an 87% selectivity to caprylic aldehyde at 270 °C, which is almost the same as the performance observed for the secondary alcohol (2-ol). Additionally, the selective oxidation of benzyl alcohol to benzaldehyde is one of the most important organic transformations, attracting enormous interest due to wide applications in the perfumery and food industries.[9,21–23] The catalytic results reported here indicate that the Ag-9/Mn_3O_4 catalyst was very reactive for the aliphatic alcohols. Benzyl alcohol was selectively oxidized to benzaldehyde with a conversion of 92% and a selectivity of 98% at 230 °C, which is just 25 °C higher than the boiling point of benzyl alcohol (205 °C). Furthermore, 1,2-propanediol (containing two hydroxyl groups) also could be oxidized to the target product with a selectivity of 74% at a conversion of 54% at 270 °C.

Considerable attention has been paid to CO oxidation over the past years because of its great significance in the treatment of exhaust gas from automobiles and for fuel cell applications.[16,24] Recently research has focused on precious metal catalysts (such as Pt, Au, and Pd), which have high activity and stability for the oxidation of CO.[25–28] Nevertheless, the high cost and limited availability of these noble metals greatly hamper the practical applications and thus activate extensive interest in the development of novel materials with excellent activity for CO oxidation prepared with inexpensive and more abundant materials.

Catalytic activity testing for CO oxidation was carried out on the as-obtained MnO_2, Ag-9/MnO_x and Ag-9/MnO_2 (Fig. 4). Clearly, we can see that Ag-9/MnO_x and Ag-9/MnO_2 are more active than the recycled MnO_2. The CO conversion reached 80% at 106 °C on Ag-9/MnO_2, at 159 °C on Ag-MnO_x and at 184 °C on recycled-MnO_2, which showed that the presence of the Ag greatly improved the catalytic activity for CO oxidation. It is noteworthy that, for Ag-9/MnO_2 and Ag/MnO_x catalysts, the temperatures required for almost 100% CO conversion are 150 °C and 180 °C respectively, while for the MnO_2 catalyst, the temperature of maximum CO conversion was 240 °C. Our results indicate that introducing Ag to MnO_2 produces an efficient catalyst for CO oxidation.

From the fact that the cyclohexanol conversion is very different over the catalysts with various supports (Ag/ZrO_2, Ag/ZnO, Ag/Al_2O_3, Ag/SiO_2, Ag/TiO_2 and Ag/Fe_2O_3), it is evident the nature of the support plays a vital role in the performance of silver for the present reaction. The XRD results have showed that MnO_2 in the fresh catalyst was transformed into Mn_3O_4 by pre-activation during the process of cyclohexanol oxidation. Similarly, XPS results showed that the surface composition of the support was transformed from MnO_2 into Mn_3O_4, and that the Ag surface remained almost unchanged (Fig. 5A and B). These results indicate that the support is an active participant for the cyclohexanol oxidation. However, for the catalyst with no silver loading, the cyclohexanol conversion was only 42% at 280 °C. The results of the control experiments showed that, for Ag catalysts on inactive supports (ZrO_2, ZnO, Al_2O_3, and SiO_2) as well as the unmodified MnO_x catalyst, the catalytic activity for alcohol oxidation was very low, while for the Ag-9/MnO_x catalyst, the activity was greatly enhanced. Similarly for the CO oxidation, Ag-9/MnO_2 showed better catalytic performance compared to the unmodified MnO_2 catalyst. For the Ag–oxide systems, several papers have focused on CO oxidation,[16,29] HCHO oxidation[30] and gas-phase selective oxidation of benzyl alcohol,[22] and they all proposed that the Ag–oxide interaction was crucial for the corresponding reactions therein. Based on our control experiments and reported results, it is proposed that strong metal–support interactions (SMSIs) exist between Ag and MnO_x. In order to verify this proposal, the used Ag-9/Mn_3O_4 was visualized by HRTEM. Interestingly, the results showed clear Ag–Mn_3O_4 interfaces (Fig. 5C and D). Other oxide–metal interfacial or perimeter sites and the SMSI therein have been known for their high activity in various reactions, such as Au–oxide[31,32] and Pt–oxide.[33–35] From the above results, it is reasonable to propose that the Ag–Mn_3O_4 interface and the interactions therein play an important or critical role in the oxidation of alcohols and CO.

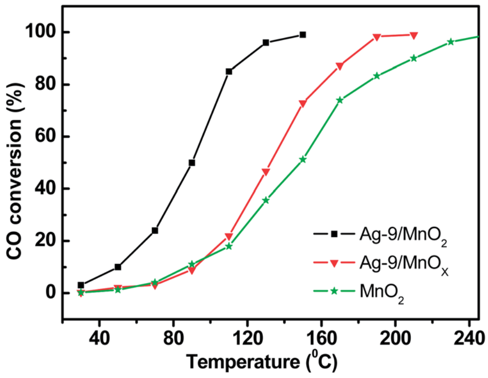

Fig. 4 Conversion–temperature curves for CO oxidation over MnO_2, Ag-9/MnO_x and Ag-9/MnO_2 catalysts.

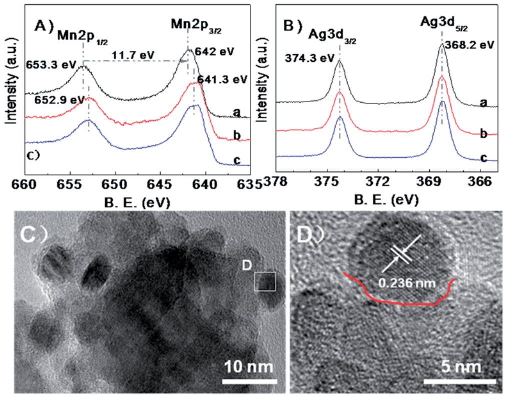

Fig. 5 (A) Mn 2p XPS spectra of (a) Ag-9/Mn_3O_4, (b) Ag-9/MnO_2 and (c) MnO_2, (B) Ag 3d XPS spectra of (a) Ag-9/Mn_3O_4, (b) Ag-9/MnO_2 and (c) Ag NPs, (C) HRTEM image of Ag-9/Mn_3O_4 catalyst. (D) HRTEM image of the region indicated with a box in panel D.

Conclusions

In summary, the used battery supported silver catalyst was successfully synthesized and showed a high catalytic performance for the gas-phase oxidation of various alcohols and CO. For cyclohexanol oxidation, Ag-9/Mn_3O_4 delivered a high conversion of 86% with a cyclohexanone selectivity of 88% at 280 °C. The high catalytic performance for the oxidation of alcohols is attributed to the synergistic effects between the Ag NPs and the Mn_3O_4 support, while the Ag–MnO_2 synergistic effect is critical for carbon dioxide formation. This study provides an example of the green-reuse of used batteries for the oxidation of alcohols and CO. Further investigations into the industrial application of this catalyst for other oxidation processes as well as the precise mechanism of the oxidation process are currently in progress.

Acknowledgements

This work was supported by the State Key Project of Fundamental Research for Nanoscience and Nanotechnology (2011CB932401, 2011CBA00500, 2012CB224802), the Foundation for the Author of National Excellent Doctoral Dissertation of P. R. China (201321), Specialized Research Fund for the Doctoral Program of Higher Education (20130002120013), and the National Natural Science Foundation of China (21221062, 21131004, 21390393, 21322107).

References

1 A. A. White, M. S. Platz, D. M. Aruguete, S. L. Jones, L. D. Madsen and R. D. Wesson, *ACS Sustainable Chem. Eng.*, 2013, **1**, 871.

2 M. J. Smith and F. M. Gray, *J. Chem. Educ.*, 2010, **87**, 162.

3 A. J. Pedersen, F. J. Frandsen, C. Riber, T. Astrup, S. N. Thomsen, K. Lundtorp and L. F. Mortensen, *Energy Fuels*, 2009, **23**, 3475.

4 T. Mallat, Z. Bodnar, P. Hug and A. Baiker, *J. Catal.*, 1995, **153**, 131.

5 A. Corma and H. Garcia, *Chem. Soc. Rev.*, 2008, **37**, 2096.

6 D. I. Enache, J. K. Edwards, P. Landon, B. Solsona-Espriu, A. F. Carley, A. A. Herzing, M. Watanabe, C. J. Kiely, D. W. Knight and G. J. Hutchings, *Science*, 2006, **311**, 362.

7 T. Mallat and A. Baiker, *Chem. Rev.*, 2004, **104**, 3037.

8 A. S. K. Hashmi, *Chem. Rev.*, 2007, **107**, 3180.

9 G. F. Zhao, H. Y. Hu, M. M. Deng, M. Ling and Y. Lu, *Green Chem.*, 2011, **13**, 55.

10 J. J. Mao, D. S. Wang, G. F. Zhao, W. Jia and Y. D. Li, *CrystEngComm*, 2013, **15**, 4806.

11 L. H. Jia, S. Zhang, F. N. Gu, Y. Ping, X. F. Guo, Z. Y. Zhong and F. B. Su, *Microporous Mesoporous Mater.*, 2012, **149**, 158.

12 H. Wu, P. Wang, H. He and Y. Jin, *Nano Res.*, 2012, **5**, 135.

13 L. C. Wang, Y. M. Liu, M. Chen, Y. Cao, H. Y. He and K. N. Fan, *J. Phys. Chem. C*, 2008, **112**, 6981.

14 L. C. Wang, X. S. Huang, Q. Liu, Y. M. Liu, Y. Cao, H. Y. He, K. N. Fan and J. H. Zhuang, *J. Catal.*, 2008, **259**, 66.

15 L. C. Wang, L. He, Q. Liu, Y. M. Liu, M. Chen, Y. Cao, H. Y. He and K. N. Fan, *Appl. Catal., A*, 2008, **344**, 150.

16 R. Xu, X. Wang, D. S. Wang, K. B. Zhou and Y. D. Li, *J. Catal.*, 2006, **237**, 426.

17 X. Yang, L. Du, S. J. Liao, Y. X. Li and H. Y. Song, *Catal. Commun.*, 2012, **17**, 29.

18 Y. Li, X. Xu, P. F. Zhang, Y. T. Gong, H. R. Li and Y. Wang, *RSC Adv.*, 2013, **3**, 10973.

19 P. Liu, Y. J. Guan, R. A. Santen, C. Li and E. J. M. Hensen, *Chem. Commun.*, 2011, **47**, 11540.

20 T. Wang, H. Shou, Y. Kou and H. C. Liu, *Green Chem.*, 2009, **11**, 562.

21 G. F. Zhao, H. Y. Hu, M. M. Deng and Y. Lu, *Chem. Commun.*, 2011, **47**, 9642.

22 M. M. Deng, G. F. Zhao, Q. S. Xue, L. Chen and Y. Lu, *Appl. Catal., B*, 2010, **99**, 222.

23 C. D. Pina, E. Falletta and M. Rossi, *J. Catal.*, 2008, **260**, 384.

24 S. J. Huang, K. J. Hara and A. Fukuoka, *Energy Environ. Sci.*, 2009, **2**, 1060.

25 H. Xu, Q. Fu, Y. X. Yao and X. H. Bao, *Energy Environ. Sci.*, 2012, **5**, 6313.

26 J. R. Gaudet, A. Riva, E. J. Peterson, T. Bolin and A. K. Datye, *ACS Catal.*, 2013, **3**, 846.

27 X. Zhang, H. Wang and B. Q. Xu, *J. Phys. Chem. B*, 2005, **109**, 9678.

28 J. W. Zhang, L. Zhang, Y. Y. Jia, G. X. Chen, X. Wang, Q. Kuang, Z. X. Xie and L. S. Zheng, *Nano Res.*, 2012, **5**, 618.

29 G. G. Xia, Y. G. Yin, W. S. Willis, J. Y. Wang and S. L. Suib, *J. Catal.*, 1999, **185**, 91.

30 Z. W. Huang, X. Gu, Q. Q. Cao, P. P. Hu, J. M. Hao, J. H. Li and X. F. Tang, *Angew. Chem., Int. Ed*, 2012, **51**, 4198.

31 M. Haruta, *CATTECH*, 2002, **6**, 102.

32 J. C. Chen, R. Y. Zhang, L. Han, B. Tu and D. Y. Zhao, *Nano Res.*, 2013, **6**, 871.

33 C. T. Campbell, *Nat. Chem.*, 2012, **4**, 597.

34 Q. Fu, W. Li, Y. Yao, H. Liu, H. Su, D. Ma, X. Gu, L. Chen, Z. Wang, H. Zhang, B. Wang and X. Bao, *Science*, 2010, **328**, 1141.

35 Q. Fu, F. Yang and X. Bao, *Acc. Chem. Res.*, 2013, **46**, 1692.